

An Artificial Neural Network Model for Downscaling of Passive Microwave Soil Moisture

SOO SEE CHAI¹, JEFFREY P WALKER², BERT VEENENDAAL³, GEOFF WEST³

¹Faculty of Computer Science and Information Technology, Universiti Malaysia Sarawak, MALAYSIA

²Faculty of Engineering, Monash University, AUSTRALIA

Department of Spatial Sciences, Curtin University of Technology, AUSTRALIA

¹sschai@fit.unimas.my, ²jeff.walker@eng.monash.edu.au, ³(b.veenendaal; g.west@curtin.edu.au)

Abstract: - In this paper, an Artificial Neural Network (ANN) model was developed to downscale the soil moisture content from low resolution L-band passive microwave observation. Using the relationship between soil evaporative efficiency derived from MODerate resolution Imaging Spectroradiometer (MODIS) and soil moisture, the ANN model was used to downscale from 20 km×20 km observation to 1 km×1 km resolution over the whole area of 40 km×40 km. The method is tested using data collected during the National Airborne Field Experiment in 2005 (NAFE'05). The soil moisture variability in term of mean and standard deviation for the pixel to be disaggregated were proposed to be used in the ANN model for downscaling purpose. In this demonstration study, soil moisture data derived from 1 km resolution from the Polarimetric L-band Multibeam Radiometer (PLMR) were aggregated to 20 km resolution pixels, and subsequently downscaled using soil moisture statistics estimated from 1 km resolution data. The overall Root Mean Square Error (RMSE) difference between the measured and predicted soil moisture values varied between 1.8% v/v and 3.5% v/v across the complete range of typically experienced soil moisture conditions. The challenge of this model for real life practicality is presented in this paper and the suggestions are made at the end of this paper.

Key-Words: - Artificial Neural Network (ANN), Passive microwave, soil moisture, downscaling

1 Introduction

Passive microwave at L-band (1.4 Ghz) has been proved to be more sensitive to soil moisture profile up to 5cm and more direct comparing to radar backscatter and thermal data [1, 2]. The Soil Moisture and Ocean Salinity (SMOS) mission, which is the first L-band soil moisture dedicated satellite launched in 2009, provides data at around 40 km resolution globally. While this spatial resolution is suitable for some broad scale applications, it is not useful for small scale applications such as on-farm water management, flood prediction or meso-scale climate and weather prediction [3]. To better utilize the low spatial resolution data, downscaling (or disaggregation) algorithms need to be matured.

For the problem of soil moisture retrieval, ancillary data are usually surface parameters which can provide valuable information. To obtain this information, field experiment will need to be conducted. Over larger area, such information might not be available. To overcome such issue, there is a choice of using statistical method, eg. Regression and the Bayes' law. With regression method, the slope of the linear law is not exactly constant from one watershed to another and calibration is needed each time when this method is applied. Bayesian method, on the other hand, requires prior probabilities distribution, which are estimated from

the training data sets, in order for the Bayes' law to find a posterior.

Compare to statistical methods, ANN has the advantages of being able to identify subtle and non-linear patterns, which is not always the case for traditional statistical methods. In addition to this, ANNs do not require normally distributed continuous data and may be used to integrate data from different source with poorly defined or unknown contributions [4].

2 Study Area and Data Set

The brightness temperature observations used in this study have been collected during the month-long NAFE field campaign held in November 2005. The campaign included extensive airborne passive microwave observations together with spatially distributed and in-situ ground monitoring of near-surface soil moisture. For the purpose of this analysis, only pertinent detail of the data will be presented. A more detailed description of the data can be obtained in [5]. The study area is situated at the northern part of the Goulburn River catchment, located in a semiarid area of south-eastern Australia. This catchment extends from 31°46'S to 32°51'S and 149°40'E to 150°36'E with elevations ranging from 106 m in the floodplains to 1257m (**Fig. 1**). The area monitored during NAFE'05 was a square area of approximately 40km×40km,

centered in the northern part of the catchment. Much of the original vegetation has been cleared to the north of the Goulburn River, where the dominant land uses are grazing and cropping. The southern part of the catchment is largely uncleared with extensive areas covered by forest. This 40km area is chosen for its moderate-to-low vegetation cover condition, and can be logistically divided into two sub-areas, the “Merriwa” area in the east and the “Krui” area in the west. The regional data measured on the 7th, 14th and 21st Nov 2005 was the target dataset for this study.

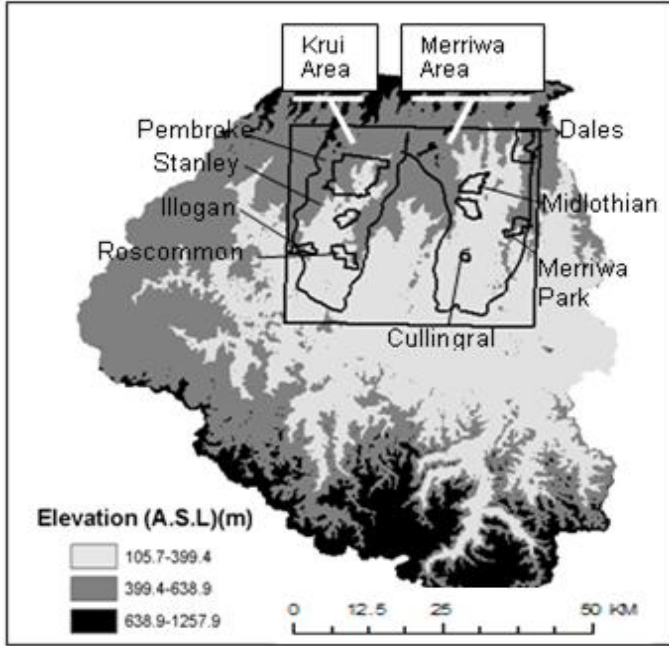


Fig. 1. Overview of NAFE'05 focus farms within Krui and Merriwa areas.

2.1 L-band derived soil moisture

Soil moisture data for the 40km×40km study area was derived at 1km nominal resolution from the L-band data using the L-MEB (L-band Microwave Emission of the Biosphere) model. A detailed description of this retrieval is presented in [6], so only pertinent details are repeated here. The 40km×40km study area was corresponding to one SMOS pixel.

Soil moisture was retrieved for each 1 km brightness temperature (T_b) pixel using the L-MEB model together with the ancillary data of land cover, soil texture, soil temperature and canopy temperature. The soil moisture output of the L-MEB algorithm was limited to a maximum soil moisture value of 58% v/v, derived from analysis of the maximum soil moisture achieved at the monitoring stations. Conversely, no lower limit was imposed on the retrieved soil moisture. The average accuracy of soil moisture retrieval at 1 km resolution using L-MEB was 3.8% v/v and in all cases better than 6% v/v over a variety of land surface conditions in the

study area [6].

2.2 MODIS data

The MODIS data used in the downscaling algorithms are composed of MODIS/Aqua Surface Reflectance Daily L2G Global 250 m and MODIS/Aqua Land Surface Temperature and Emissivity Daily L3 Global 1 km products. The MODIS NDVI (Normal Difference Vegetation Index) was calculated using Band 1 and Band 2 of the MODIS/Aqua Surface Reflectance L2G Global 250 m product. The MODIS/Aqua data were selected since there is no significant discrepancies between the NDVI values derived from Terra and Aqua satellites of MODIS [7] and all the data during the regional observations were available from this satellite. The NDVI was derived from cloud-free products. During the three regional observations dates (7th Nov 2005, 14th Nov 2005 and 21st Nov 2005), the MODIS surface temperatures images were not totally cloud free, each with 31%, 13% and 15% cloud cover respectively.

3 Methodology

In this paper, the linear downscaling relationship by [8] is applied in the ANN model. Based on data available from MODIS and physical based model predictions of soil evaporative efficiency derived from MODIS surface temperature and NDVI, [8] developed a deterministic model for downscaling soil moisture from SMOS scaled observations according to:

$$\theta = \theta_{SMOS} + \theta_C SMP_{MODIS} \quad (1)$$

where, θ : downscaled soil moisture,

θ_{SMOS} : SMOS-scale soil moisture,

$$SMP_{MODIS} = \frac{T_{SMOS} - T_{MODIS}}{T_{MODIS} - T_{min}} \quad (2)$$

with T_{MODIS} : soil skin temperature derived from MODIS data at the time of interest, T_{SMOS} : the areal average of T_{MODIS} and T_{min} : soil temperature at maximum soil moisture,

The characteristic volume fraction, θ_C , of water is computed as:

$$\theta_C = \theta_{c0} (1 + \gamma / r_{ah}) \quad (3)$$

where, θ_{c0} (% v/v) and γ ($s \ m^{-1}$) being two soil dependent parameters and r_{ah} ($s \ m^{-1}$) the aerodynamic resistance over bare soil, given the roughness and the wind speed. The empirical parameter θ_{c0} controls the soil capacity to retain moisture in optimal evaporative condition, i.e. when wind speed is zero or r_{ah} is infinite. In other words, the higher the θ_{c0} , the slower the soil dries. θ_C is the most important parameter to be estimated [8].

3.1 ANN downscaling approach

In this study, ANN is used to learn the relationship between θ , θ_{SMOS} and SMP_{MODIS} without the value of θ_C , which is not available directly from the data of the field experiment used, and maps a function between these three variables through the learning process during ANN training. An analogy for this phenomena is a set of data of a function $y = mx + 3$. For a particular situation, let the value of $m = 2$. By supplying the values of x and the value 3 as the inputs, and the calculated y values for the corresponding x values, the ANN can map a function between the inputs and output using a linear model. This simple scenario becomes more complicated when m is a parameter, which is dependent on other factors, i.e. the value of m will change. The value of θ_C is related to wind speed and two soil dependent parameters, and hence the “complicated” scenario in the analogy happens when this linear relationship is adopted in the ANN model without having the value of θ_C . To account the variability of θ_C , the mean and standard deviation of soil moisture at a finer resolution is used. This is explained in detailed in Section 3.1.2.

3.1.1 Data preparation

The data on 7th Nov 2005 is selected for the training of the ANN model. To increase the number of data for this demonstration, the 40 km×40 km area is divided into many 20 km×20 km grids. A total of seven 20 km areas are randomly selected. After the ANN model manages to build a relationship with the lowest Root Mean Square Error (RMSE), this ANN model is tested with data on 14th and 21st Nov 2005. On each of these dates, four 20 km×20 km grids are used.

3.1.2 Spatial variability of soil moisture

To account for the unavailability of the most important parameter θ_C in equation (1), the variability of this variable is “approximated” using the mean and standard deviation of the soil moisture values at a finer resolution. In this demonstration study, this is done by calculating the mean and standard deviation soil moisture values from the 1 km soil moisture data, described in Section 2.1. For real-life application, these values could be approximate from radar data which offers higher resolution data. The mean and standard deviation of the soil moisture data are used for the normalization and de-normalization of the soil moisture values. In a study by [9], standard deviation was used as an indicator for selection of similarity data between the training and testing data in order to achieve a good

retrieval accuracy. The study by [9] had limited the use of ANN for time and site specific purpose, which would not be very useful when the retrieval is needed to be done covering a wider range of time scale, as shown in this demonstration study.

4 Results and Discussion

4.1 ANN architecture

The inputs of the ANN are θ_{SMOS} and SMP_{MODIS} , while the output is θ . The number of nodes in the input and output layers are determined by the number of input and output parameters. However, a decision needs to be made regarding the number of hidden layers and the number of hidden neurons in each of the hidden layers. There is currently no theoretical reason to use neural networks with more than two hidden layers [10]. For this reason, the ANN architecture being determined has either one or two hidden layers. Using too few or too many hidden neurons may undermine the application. Too few hidden neurons will cause underfitting to occur, whereby complicated signals within the data are poorly represented by simple models in the ANN. On the other hand, using too many hidden neurons will cause overfitting whereby the neural network has too much information processing capacity to build complex models, such that the limited amount of information contained in the training set is not enough to train all of the neurons in the hidden layers. Moreover, if too many hidden neurons are used, the amount of training time will increase. Currently, the best way to optimize the number of hidden layers and the number of hidden neurons is simply through trial and error [11].

The Broyden-Fletcher-Goldfarb-Shanno (BFGS) training algorithm chosen was based on the previous study in [12].

4.2 Window size selection

As the surface soil moisture variance observed within a square metre can be as large as a whole field [13], there is a need to determine the size of the area (hereafter, referred as “window”) whereby the ANN can capture better the spatial variability within this smaller region comparing to the 20 km×20 km grid. The mean and standard deviation of the soil moisture values within the windows are calculated. Within the 20 km×20 km grid, the prediction of the soil moisture at 1 km is done within the selected window size. The prediction is next moved to the window that is to the right of this current window, i.e. prediction will be done from left to right, top to bottom within the 20 km×20 km grid.

To select the optimum window size, the sizes of: 2 km×2 km, 3 km×3 km, 4 km×4 km and 5 km×5 km are used (hereafter these sizes are known as window). A sub-set of data on 7th Nov 2005 is used for this purpose.

The cells of the smaller grids are the sub-sets of the bigger grids. For example, the grid of 2 km×2 km is the sub-sets of the other windows (Fig. 2). With such relationships, the variances of the results obtained, if any, are caused by the new cells in the larger window. Moreover, the new cells added in the larger windows are close to the smaller sub-set of the larger window. The topography, land uses, and soil texture conditions of the new cells are expected to be similar to those for the smaller sub-sets.

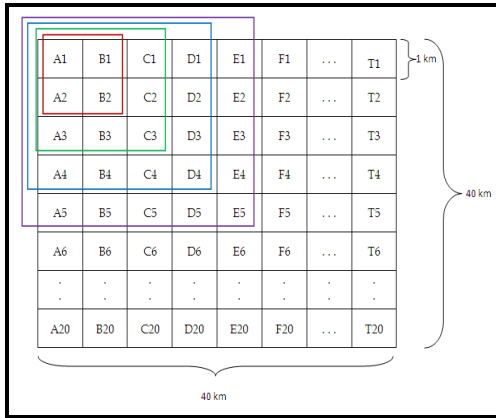


Fig.2. The different window sizes used for the purpose of selecting the optimum window size.

4.3 Optimum ANN architecture and window size

For the one hidden layer, number of hidden neurons being tested are: 2, 4, 6, 8, 10, 20, 50, 100 while for two hidden layers, each hidden layer with the same hidden neurons of: 2, 4, 5, 10, 20. Note: for two hidden layers, notation 2:2, 3:3, ..., are used.

From Tab. 1, it can be seen that, the prediction results deteriorate as the window size increases. For example, for single layer of two hidden neurons, the RMSE values deteriorate from 4.09% v/v for 2km×2km grid to 4.69%v/v at 3km×3km, to 6.47%v/v and 6.48%v/v for 4km×4km and 5km×5km, respectively. This is as expected, as for a bigger window size, the soil moisture variance will be higher comparing to a smaller window size because of a lack of homogeneity. As the variance increases, the ANN is unable to capture this variability, causing the retrieval accuracy to deteriorate. For a single hidden layer of 10 neurons, the best RMSE obtained is 3.56% v/v with a correlation coefficient, $R^2 = 0.46$ for the 2km×2km “window” size. For two hidden layers of 10 neurons in each layer, it is 3.67% v/v with $R^2 = 0.40$ for the 2km×2km window. The results show that the use of two hidden layers gives little improvement in the accuracy of predictions, indicating that a more complex model is unnecessary. In addition to this, when the window size increases, the RMSE values increase.

The lowest RMSE (3.56% v/v) was obtained with one hidden layer of 10 neurons and at window of 2 km×2 km.

4.4 Evaluation cases

With this architecture (number of neurons and hidden layer) and the size of the window defined, this methodology is evaluated using the data of the 14th and 21st Nov 2005.

Using this methodology, the RMSE between the actual and predicted values for each of the four grids of 20 km×20 km on the 14th and 21st Nov 2005 are shown in Tab. 2. It can be seen that the RMSE values range from 1.8% v/v to 3.5% v/v. The correlations of the actual and predicted soil moisture are shown using scatter plots in Fig. 3. The actual and predicted soil moisture maps shown in Fig. 4 show reasonable correspondence between the actual and predicted maps. From the spatial difference of the soil moisture map, generally, the predicted soil moisture using this methodology is slightly lower compared to the actual soil moisture as evidenced by the large number of cells of positive difference.

5.0 Conclusions

This demonstration work has shown that the ANN is able to downscale from 20 km brightness temperature data to 1 km soil moisture data with encouraging accuracy, provided that the spatial variability of soil moisture data, i.e. the mean and standard deviation data, at 2 km×2 km can be obtained. The main benefit of this methodology is in term of the minimum number of input data required. In this approach, besides the mean and standard deviation of the soil moisture data at 2 km×2 km, only the θ_{SMOS} and SMP_{MODIS} , which can be obtained from satellites, are used as input variables. One possible solution in obtaining the mean and standard deviation could be using radar data which provides higher resolution data.

Acknowledgement

The National Airborne Field Experiments have been made possible through recent infrastructure (LE0453434 and LE0560930) and research (DP0557543) funding from the Australia Research Council, and the collaboration of a large number of scientists from throughout Australia, the United States and Europe. Special thanks are also due to the Malaysian Ministry of Higher Education for the PhD scholarship of Soo See Chai. Part of this research project is registered as non-funded research under Universiti Malaysia Sarawak (NF(F08)/155/2011(03)).

References:

- Kerr, Y., *Soil moisture from space: Where are we?* Hydrogeology journal, 2007. **15**(1): p. 117-120.
- Wagner, W., G. Bloschl, P. Pampaloni, J. Calvet, B. Bizzarri, J. Wigneron, and Y. Kerr, *Operational readiness of microwave remote sensing of soil moisture for hydrologic applications*. Nordic hydrology, 2007. **38**(1): p. 1-20.
- Walker, J.P. and R. Panciera, *National Airborne Field Experiment 2005: Experiment Plan*. 2005, Department of Civil and Environmental Engineering, The University of Melbourne.
- Notarnicola, C., M. Angiulli, and F. Posa, *Soil Moisture Retrieval From Remotely Sensed Data: Neural Network Approach Versus Bayesian Method*. IEEE Transactions on Geoscience and Remote Sensing, 2008. **46**(2): p. 547-557.
- Panciera, R., J.P. Walker, J.D. Kalma, E.J. Kim, J.M. Hacker, O. Merlin, M. Berger, and N. Skou, *The NAFE'05/CoSMOS Data Set: Toward SMOS Soil Moisture Retrieval, Downscaling, and Assimilation*. IEEE Transactions on Geoscience and Remote Sensing, 2008. **46**(3): p. 736-745.
- Panciera, R., *Effect of Land Surface Heterogeneity on Satellite Near-surface Soil Moisture Observations (Phd Thesis in preparation)*, in Dept. of Civil and Environmental Engineering. 2009, The University of Melbourne: Melbourne.
- Jing, W., G. Ni, W. Xiaoping, and Y. Jia. *Comparisons of normalized difference vegetation index from MODIS Terra and Aqua data in northwestern China*. in *IEEE International Geoscience and Remote Sensing Symposium, 2007. IGARSS 2007*. 2007.
- Merlin, O., J.P. Walker, A. Chehbouni, and Y. Kerr, *Towards deterministic downscaling of SMOS soil moisture using MODIS derived soil evaporative efficiency*. Remote Sensing of Environment, 2008. **112**(10): p. 3935-3946.
- Chai, S., B. Veenendaal, G. West, and J. Walker. *Input Pattern According to Standard Deviation of Backpropagation Neural Network: Influence on Accuracy of Soil Moisture Retrieval*. in *IEEE International Geoscience and Remote Sensing Symposium (IGARSS)*. 2008. Boston, Massachusetts, U.S.A.: IEEE.
- Heaton, J., *Introduction to Neural Networks for Java*. 2008: Heaton Research Inc.
- Lakhankar, T., *Estimation of soil moisture using microwave remote sensing data*. 2006.
- Chai, S., B. Veenendaal, G. West, and J. Walker, *Backpropagation Neural Network For Soil Moisture Retrieval Using Nafe'05 Data: A Comparison Of Different Training Algorithms*. Int Archives Photogramm, Remote Sens Spatial Inf Sci (China), 2008. **37**: p. 1345.
- Van Oevelen, P., *Soil moisture variability: a comparison between detailed field measurements and remote sensing measurement techniques/Variabilité de l'humidité du sol: une comparaison entre des mesurages détaillés des champs et les mesurages réalisés par télédétection*. Hydrological Sciences Journal, 1998. **43**(4): p. 511-520.

Tab. 1. The effects of using different architecture and window sizes.

	Hidden Neuron	RMSE (%v/v) (R ²) for Different Window Sizes			
		2×2 km	3×3 km	4×4 km	5×5 km
One Layer	2	4.09 (0.29)	4.69 (0.22)	6.47 (0.05)	6.48 (0.12)
	4	4.07 (0.55)	4.84 (0.20)	6.50 (0.002)	6.52 (0.02)
	6	3.89 (0.54)	4.84 (0.15)	6.60 (0.20)	6.49 (0.0002)
	8	3.80 (0.55)	4.76 (0.18)	6.56 (7.3E-06)	6.51 (0.02)
	10	3.56 (0.46)	4.59 (0.22)	6.45 (0.003)	6.21 (0.02)
	20	5.55 (0.13)	6.24 (0.18)	7.43 (0.13)	7.42 (0.13)
	50	6.02 (0.12)	6.93 (0.24)	6.31 (1E-08)	6.31 (0.12)
	100	5.08 (0.26)	5.77 (0.26)	6.37 (0.10)	6.60 (0.14)
Two Layers	2:2	4.44 (0.17)	4.90 (0.25)	6.48 (0.09)	6.57 (0.13)
	4:4	3.84 (0.38)	4.49 (0.27)	6.64 (0.08)	6.69 (0.11)
	5:5	5.00 (0.11)	5.63 (0.15)	6.66 (0.10)	6.88 (0.04)
	10:10	3.67 (0.40)	4.46 (0.27)	6.54 (0.05)	6.62 (0.05)
	20:20	4.67 (0.04)	5.33 (0.19)	6.37 (0.11)	6.49 (0.14)

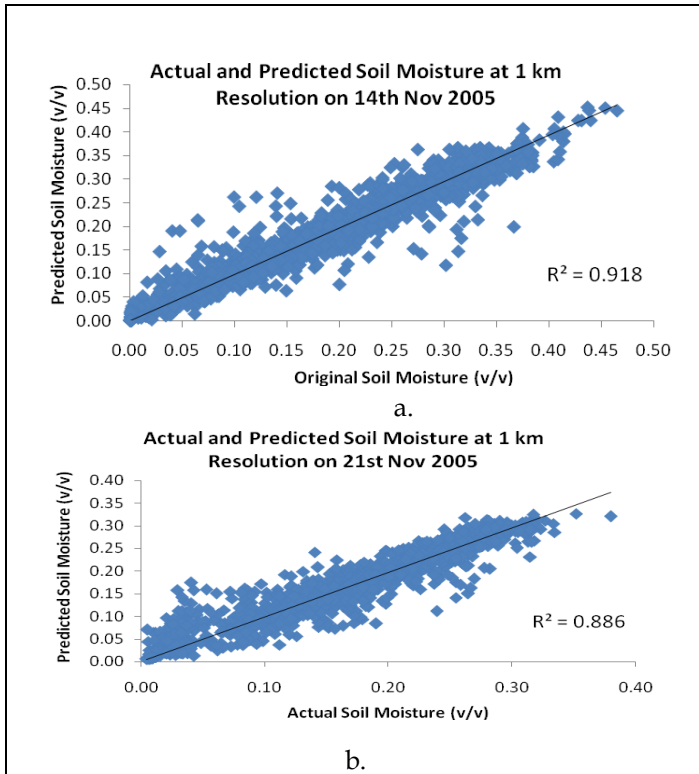


Fig. 3. The actual and predicted soil moisture values after applying the downscaling methodology.

Tab. 2. The RMSE values obtained for each 20 km×20 km grids.

Date	Grid (20 km×20 km)	RMSE (%v/v)
14 th Nov 2005	Grid 1	3.5
	Grid 2	3.4
	Grid 3	2.3
	Grid 4	1.8
21 st Nov 2005	Grid 1	2.7
	Grid 2	2.9
	Grid 3	2.0
	Grid 4	2.3

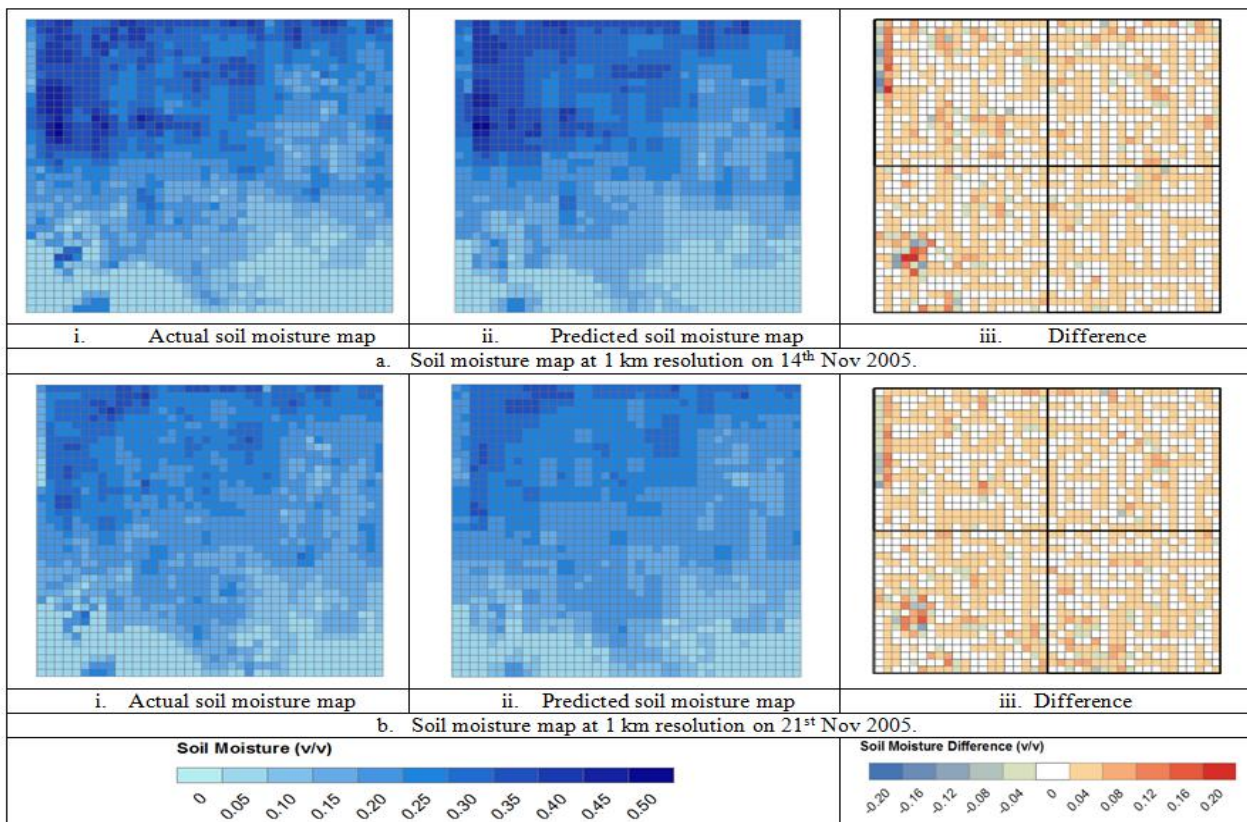


Fig. 4. The actual and predicted soil moisture maps at 1 km resolution after applying the downscaling methodology. The difference between the actual and predicted soil moisture for each date is also shown.